Journal of Zhejiang University SCIENCE A
ISSN 1673-565X (Print); ISSN 1862-1775 (Online)
www.zju.edu.cn/jzus; www.springerlink.com
E-mail: jzus@zju.edu.cn

3D thermoelasticity solutions for functionally graded thick plates*

Ji YING[1], Chao-feng LÜ†‡[2], C. W. LIM[3]

([1]*Department of Mechanical Engineering, Zhejiang University, Hangzhou 310027, China*)

([2]*Department of Civil Engineering, Zhejiang University, Hangzhou 310058, China*)

([3]*Department of Building and Construction, City University of Hong Kong, Hong Kong, China*)

†E-mail: lucf@zju.edu.cn

Received May 28, 2008; Revision accepted Nov. 6, 2008; Crosschecked Jan. 9, 2009

Abstract: Thermal-mechanical behavior of functionally graded thick plates, with one pair of opposite edges simply supported, is investigated based on 3D thermoelasticity. As for the arbitrary boundary conditions, a semi-analytical solution is presented via a hybrid approach combining the state space method and the technique of differential quadrature. The temperature field in the plate is determined according to the steady-state 3D thermal conduction. The Mori-Tanaka method with a power-law volume fraction profile is used to predict the effective material properties including the bulk and shear moduli, while the effective coefficient of thermal expansion and the thermal conductivity are estimated using other micromechanics-based models. To facilitate the implementation of state space analysis through the thickness direction, the approximate laminate model is employed to reduce the inhomogeneous plate into a homogeneous laminate that delivers a state equation with constant coefficients. The present solutions are validated by comparisons with the exact ones for both thin and thick plates. Effects of gradient indices, volume fraction of ceramics, and boundary conditions on the thermomechanical behavior of functionally graded plates are discussed.

Key words: Functionally graded plates, Semi-analytical solutions, 3D thermoelasticity, Mori-Tanaka method
doi:10.1631/jzus.A0820406 **Document code:** A **CLC number:** O34

INTRODUCTION

The concept of functionally graded materials (FGMs) was proposed in the early 1980s by materials scientists in Japan as a means of preparing thermal barrier materials (Koizumi, 1997). Along with the development of the manufacturing techniques for FGMs and its increasing applications in engineering, including armor plating, heat engine components, gas turbines, aircrafts fuselages, and human implants, etc., a great many approaches have been developed during the past years to investigate thermomechanical behavior of FGM plates, among which the 2D deformable theories, such as the higher-order deformable theory (Reddy, 2000; Matsunaga, 2008), the self-consistent refined theory (Bian *et al*., 2005), and the 3D elasticity solutions (Tarn and Wang, 1995; Mian and Spencer, 1998; Cheng and Batra, 2000; Chen *et al*., 2003b) are popular ones. In the 2D deformable theories, the boundary conditions on the edges of the plate are applied in an average sense, and hence these theories are only applicable to moderately thick plates. Moreover, the 2D theories belong to the global method in which the deformation rigidities are present in the form of the integral of the coordinate-dependent elastic constants. Hence, when it comes to the local responses, such as the stresses or strains at a special point in strongly thick plates especially where the material properties vary abruptly, the accuracy of 2D theories is always inadequate for engineering applications. The 3D elasticity theory makes no assumption about the deformation field, but directly uses the stress and strain or displacement throughout the analysis. Hence, 3D theory is widely preferred when analyzing FGM plates.

‡ Corresponding author

* Project supported by the National Natural Science Foundation of China (Nos. 10702061, 10725210, and 10832009), and Zhejiang Provincial Natural Science Foundation of China (No. Y607116)

Tarn and Wang (1995) proposed the method of asymptotic expansion for 3D analyses of thermomechanical deformations of inhomogeneous plates. They obtained sets of recurrence equations that can be integrated successively to determine the solution for the considered problem and assessed that the classical laminated plate theory is merely the leading-order approximation in the asymptotic theory. The asymptotic expansion was later applied by many researchers to obtain 3D analytical solutions for the thermoelastic deformation of FGM elliptic and rectangular plates (Cheng and Batra, 2000; Reddy and Cheng, 2001; Vel and Batra, 2002; 2003). Mian and Spencer (1998) presented an exact 3D solution for FGM plates by solving the 2D classical equations for stretching and bending of an "equivalent plate" with elastic constants that are an appropriate weighted average of that of the FGM plates. Chen *et al.*(2003b) developed a 3D thermomechanical analysis using the state space method (SSM) for fully simply supported FGM plates, where the approximate laminate model (ALM) was introduced to treat arbitrary variations of material properties through the thickness. The SSM was also applied by Zhong and Shang (2003; 2005) to give exact 3D solutions for fully simply supported FGM piezoelectric plates with material properties varying exponentially through the thickness. Kashtalyan (2004) obtained an exact solution for FGM plates, also with exponential variations, making use of the Plevako general solution for the equilibrium equations. However, in most of the previous 3D analytical analyses for rectangular plates, displacement and stress components were expanded into Fourier series relating to the in-plane coordinates, hence restricted to fully simply supported plates. When it comes to a plate with at least one edge not constrained by a simple support, such Fourier series are no longer applicable and numerical techniques should be resorted to.

Here, the abovementioned SSM is employed to derive a state equation in partial differential form with respect to the thickness coordinate based on the 3D thermoelasticity. Then the generalized differential quadrature method (DQM) (Bellman and Casti, 1971; Shu, 2000) is introduced to derive a series of ordinary differential state equations at arbitrary discrete points, thus a semi-analytical solution is attainable. The boundary constraint conditions are incorporated by virtue of the variables at the edge points, making it possible to treat arbitrary boundary conditions other than simple supports. This combined use of SSM and DQM was pioneered by Chen *et al.*(2003a; 2004) for laminated beams with subsequent applications for laminated plates (Chen and Lüe, 2005; Lü *et al.*, 2007) and functionally graded beams (Lü and Chen, 2005; Lü *et al.*, 2006; 2008). The method allows precise treatment of edge boundary conditions point by point along the thickness direction and hence the Saint-Venant principle is not necessary any more.

In the present study, the effective bulk and shear moduli of the FGM plates are predicted according to the Mori-Tanaka method (Mori and Tanaka, 1973), while the effective coefficient of thermal expansion and the thermal conductivity are estimated by the micromechanics-based models of Rosen and Hashin (1970)'s and Hatta and Taya (1985)'s, respectively. The temperature field, which is determined according to the 3D steady-state thermal conduction, along with the elastic field through the thickness domain, is treated using the SSM. The present method is validated by comparing numerical results to the analytical 3D solutions using other methods. The current semi-analytical solutions, especially for those with strongly thick geometries and non-simple supports, are expected to provide benchmarks for future numerical analyses.

DISCRETIZED STATE SPACE FORMULATIONS

Consider an isotropic FGM plate having the length a, width b, thickness h, Young's modulus E, Poisson's ratio ν, and coefficient of thermal expansion α. The Cartesian coordinate system (x, y, z) is established such that $0\leq x\leq a$, $0\leq y\leq b$, and $0\leq z\leq h$. The plate is simply supported at the two opposite edges of $y=0$ and $y=b$, but constrained arbitrarily at the other two edges. For isotropic materials, the 3D Duhamel-Neumann relations are given by (Ding *et al.*, 2006):

$$\sigma_x = C\left(\frac{\partial u}{\partial x}+\nu\frac{\partial v}{\partial y}+\nu\frac{\partial w}{\partial z}\right)-\beta T,\ \tau_{yz}=\mu\left(\frac{\partial w}{\partial y}+\frac{\partial v}{\partial z}\right),$$

$$\sigma_y = C\left(\nu\frac{\partial u}{\partial x}+\frac{\partial v}{\partial y}+\nu\frac{\partial w}{\partial z}\right)-\beta T,\ \tau_{xz}=\mu\left(\frac{\partial w}{\partial x}+\frac{\partial u}{\partial z}\right),$$

$$\sigma_z = C\left(\nu\frac{\partial u}{\partial x}+\nu\frac{\partial v}{\partial y}+\frac{\partial w}{\partial z}\right)-\beta T,\ \tau_{xy}=\mu\left(\frac{\partial v}{\partial x}+\frac{\partial u}{\partial y}\right), \tag{1}$$

where σ_i and σ_{ij} are the normal and shear stress components, respectively; u, v, and w are the displacement components in x, y, and z directions, respectively; $C=E/(1-\nu^2)$, $\beta=(1+2\nu)C\alpha$, $\mu=E/2(1+\nu)$; and T is the temperature rise relative to the stress-free reference configuration. In the absence of body forces, the governing equations of equilibrium are expressed as

$$\begin{aligned}&\frac{\partial\sigma_x}{\partial x}+\frac{\partial\tau_{xy}}{\partial y}+\frac{\partial\tau_{xz}}{\partial z}=0,\\&\frac{\partial\tau_{xy}}{\partial x}+\frac{\partial\sigma_y}{\partial y}+\frac{\partial\tau_{yz}}{\partial z}=0,\\&\frac{\partial\tau_{xz}}{\partial x}+\frac{\partial\tau_{yz}}{\partial y}+\frac{\partial\sigma_z}{\partial z}=0.\end{aligned} \tag{2}$$

Since the plate is simply supported along the pair of opposite edges at $y=0$ and $y=b$, all variables are sought in the form of Lévy-type solutions as

$$\begin{aligned}&\begin{Bmatrix}\sigma_z\\u\\v\\w\\\tau_{xz}\\\tau_{yz}\end{Bmatrix}=\sum_{m=1}^{\infty}\begin{Bmatrix}\mu_0 Z(\xi,\zeta)\sin(m\pi\eta)\\hU(\xi,\zeta)\sin(m\pi\eta)\\hV(\xi,\zeta)\cos(m\pi\eta)\\hW(\xi,\zeta)\sin(m\pi\eta)\\\mu_0\Gamma_{xz}(\xi,\zeta)\sin(m\pi\eta)\\\mu_0\Gamma_{yz}(\xi,\zeta)\cos(m\pi\eta)\end{Bmatrix},\\&\begin{Bmatrix}\sigma_x\\\sigma_y\\\tau_{xy}\end{Bmatrix}=\mu_0\sum_{m=1}^{\infty}\begin{Bmatrix}X(\xi,\zeta)\sin(m\pi\eta)\\Y(\xi,\zeta)\sin(m\pi\eta)\\\Gamma_{xy}(\xi,\zeta)\cos(m\pi\eta)\end{Bmatrix},\end{aligned} \tag{3}$$

where X, Y, Z, Γ_{xy}, Γ_{xz}, and Γ_{yz} are non-dimensional stress components; U, V, and W are the non-dimensional displacement components; $\xi=x/a$, $\eta=y/b$, and $\zeta=z/h$ are the non-dimensional coordinates; m is an integer; and μ_0 is the shear modulus at the surface of $\zeta=0$. For the sake of analytical solutions, the temperature rise T in Eq.(1) is expanded into a Fourier series similar to Eq.(3) as follows:

$$T(\xi,\eta,\zeta)=\sum_{m=1}^{\infty}t_0(\xi,\zeta)\sin(m\pi\eta), \tag{4}$$

where the Fourier coefficient is determined by $t_0(\xi,\zeta)=2\int_0^1 T(\xi,\eta,\zeta)\sin(m\pi\eta)\mathrm{d}\eta$. Substituting Eqs.(3) and (4) into Eqs.(1) and (2), the following state equation is obtained:

$$\frac{\partial}{\partial\zeta}\begin{Bmatrix}\boldsymbol{\delta}_1\\\boldsymbol{\delta}_2\end{Bmatrix}=\begin{bmatrix}\mathbf{0}&\mathbf{A}_1\\\mathbf{A}_2&\mathbf{0}\end{bmatrix}\begin{Bmatrix}\boldsymbol{\delta}_1\\\boldsymbol{\delta}_2\end{Bmatrix}+\begin{Bmatrix}\mathbf{0}\\\boldsymbol{\theta}\end{Bmatrix}t_0(\xi,\zeta), \tag{5}$$

where

$$\boldsymbol{\delta}_1=\begin{Bmatrix}Z\\U\\V\end{Bmatrix},\ \boldsymbol{\delta}_2=\begin{Bmatrix}W\\\Gamma_{xz}\\\Gamma_{yz}\end{Bmatrix},\ \mathbf{A}_1=\begin{bmatrix}0&-\bar{l}_a\partial_\xi&\bar{l}_m\\-\bar{l}_a\partial_\xi&\bar{\mu}^{-1}&0\\-\bar{l}_m&0&\bar{\mu}^{-1}\end{bmatrix},$$

$$\mathbf{A}_2=\begin{bmatrix}(1-\nu)/(2\bar{\mu})&-\nu\bar{l}_a\partial_\xi&\nu\bar{l}_m\\-\nu\bar{l}_a\partial_\xi&-\bar{E}\bar{l}_a^2\partial_\xi^2+\bar{\mu}\bar{l}_m^2&(1+2\nu)\bar{\mu}\bar{k}_a\bar{l}_m\partial_\xi\\-\nu\bar{l}_m&-(1+2\nu)\bar{\mu}\bar{l}_a\bar{l}_m\partial_\xi&-\bar{\mu}\bar{l}_a^2\partial_\xi^2+\bar{E}\bar{l}_m^2\end{bmatrix},$$

$$\boldsymbol{\theta}=\begin{Bmatrix}1\\2\bar{\mu}\bar{l}_a\partial_\xi\\2\bar{\mu}\bar{l}_m\end{Bmatrix}(1+2\nu)\alpha,\ \partial_\xi=\frac{\partial}{\partial\xi},\ \partial_\xi^2=\frac{\partial^2}{\partial\xi^2},$$

in which $\bar{l}_a=h/a$ and $\bar{l}_m=m\pi h/b$. Here, an over-bar represents the non-dimensional elastic constants normalized by μ_0. The six variables in Eq.(5) are termed the state variables, in terms of which the induced variables are given by

$$\begin{aligned}\begin{Bmatrix}X\\Y\\\Gamma_{xy}\end{Bmatrix}=&\begin{bmatrix}\nu&\bar{E}\bar{l}_a\partial_\xi&-2\nu\bar{\mu}\bar{l}_m\\\nu&2\nu\bar{\mu}\bar{l}_a\partial_\xi&-\bar{E}\bar{l}_m\\0&\bar{\mu}\bar{l}_m&\bar{\mu}\bar{l}_a\partial_\xi\end{bmatrix}\begin{Bmatrix}Z\\U\\V\end{Bmatrix}\\&-\begin{Bmatrix}1\\1\\0\end{Bmatrix}2(1+2\nu)\bar{\mu}\alpha t_0(\xi,\zeta).\end{aligned} \tag{6}$$

To obtain the solution of Eq.(5), the technique of differential quadrature (DQ) (Shu, 2000) is adopted to approximate the derivatives with respect to ξ. Hence, a system of ordinary differential state equations at an arbitrary discrete point ξ_i is readily obtained. An assembly of the state equations at all the discrete points gives rise to the following state equation in a global

transfer matrix form,

$$\frac{\mathrm{d}\boldsymbol{\Delta}}{\mathrm{d}\zeta}=\boldsymbol{M}\boldsymbol{\Delta}+\boldsymbol{\Theta}\boldsymbol{t}_0(\zeta), \tag{7}$$

where

$$\boldsymbol{\Delta}=\begin{Bmatrix}\boldsymbol{\Delta}_1\\ \boldsymbol{\Delta}_2\end{Bmatrix},\ \boldsymbol{\Delta}_1=\begin{Bmatrix}\boldsymbol{Z}\\ \boldsymbol{U}\\ \boldsymbol{V}\end{Bmatrix},\ \boldsymbol{\Delta}_2=\begin{Bmatrix}\boldsymbol{W}\\ \boldsymbol{\Gamma}_{xz}\\ \boldsymbol{\Gamma}_{yz}\end{Bmatrix},\ \boldsymbol{M}=\begin{bmatrix}\boldsymbol{0} & \boldsymbol{M}_{\mathrm{U}}\\ \boldsymbol{M}_{\mathrm{L}} & \boldsymbol{0}\end{bmatrix},$$

$$\boldsymbol{M}_{\mathrm{U}}=\begin{bmatrix}\boldsymbol{0} & -l_a\boldsymbol{g}^{(1)} & l_m\boldsymbol{I}\\ -l_a\boldsymbol{g}^{(1)} & \bar{\mu}^{-1}\boldsymbol{I} & \boldsymbol{0}\\ -l_m\boldsymbol{I} & \boldsymbol{0} & \bar{\mu}^{-1}\boldsymbol{I}\end{bmatrix},$$

$$\boldsymbol{M}_{\mathrm{L}}=\begin{bmatrix}(1-\nu)\boldsymbol{I}/(2\bar{\mu}) & -\nu l_a\boldsymbol{g}^{(1)} & \nu l_m\boldsymbol{I}\\ -\nu l_a\boldsymbol{g}^{(1)} & -\bar{E}l_a^2\boldsymbol{g}^{(2)}+\bar{\mu}l_m^2\boldsymbol{I} & (1+2\nu)\bar{\mu}l_al_m\boldsymbol{g}^{(1)}\\ -\nu l_m\boldsymbol{I} & -(1+2\nu)\bar{\mu}l_al_m\boldsymbol{g}^{(1)} & -\bar{\mu}l_a^2\boldsymbol{g}^{(2)}+\bar{E}l_m^2\boldsymbol{I}\end{bmatrix},$$

$$\boldsymbol{\Theta}=\begin{Bmatrix}\boldsymbol{0}\\ \boldsymbol{\Theta}_{\mathrm{L}}\end{Bmatrix},\ \boldsymbol{\Theta}_{\mathrm{L}}=(1+2\nu)\alpha\begin{Bmatrix}\boldsymbol{I}\\ 2\bar{\mu}l_a\boldsymbol{g}^{(1)}\\ 2\bar{\mu}l_m\boldsymbol{I}\end{Bmatrix},$$

where $\boldsymbol{X}$, $\boldsymbol{Y}$, $\boldsymbol{Z}$, $\boldsymbol{\Gamma}_{xz}$, $\boldsymbol{\Gamma}_{yz}$, $\boldsymbol{U}$, $\boldsymbol{V}$, and $\boldsymbol{W}$ are vectors composed of the non-dimensional physical quantities defined in Eq.(3) at all discrete points along the x-direction, $\boldsymbol{t}_0$ is the temperature vector composed of temperature components at all discrete points, $\boldsymbol{g}^{(n)}$ is the weighting coefficient matrix (Shu, 2000), and $\boldsymbol{I}$ is the unity matrix of dimension $N\times N$, with N denoting the total number of discrete points along the x-direction. Similarly, the in-plane stresses (induced variables) at all discrete points are obtained as

$$\begin{Bmatrix}\boldsymbol{X}\\ \boldsymbol{Y}\\ \boldsymbol{\Gamma}_{xy}\end{Bmatrix}=\begin{bmatrix}\nu\boldsymbol{I} & \bar{E}l_a\boldsymbol{g}^{(1)} & -2\nu\bar{\mu}l_m\boldsymbol{I}\\ \nu\boldsymbol{I} & 2\nu\bar{\mu}l_a\boldsymbol{g}^{(1)} & -\bar{E}l_m\boldsymbol{I}\\ 0 & \bar{\mu}l_m\boldsymbol{I} & \bar{\mu}l_a\boldsymbol{g}^{(1)}\end{bmatrix}\begin{Bmatrix}\boldsymbol{Z}\\ \boldsymbol{U}\\ \boldsymbol{V}\end{Bmatrix}-\begin{Bmatrix}1\\ 1\\ 0\end{Bmatrix}2(1+2\nu)\bar{\mu}\alpha\boldsymbol{I}\boldsymbol{t}_0(\zeta). \tag{8}$$

For a special problem, all constraint conditions at the edges of ξ=0 and ξ=1 must be incorporated into the state equation so as to obtain a unique solution to Eq.(7). Since some specific state variables can be obtained from the boundary conditions either in the form of algebraic expressions of other state variables or known values (zero), the differential equations of these state variables in Eq.(7) should be eliminated (Chen and Lüe, 2005). After incorporating all boundary conditions into Eq.(7), the unique-solution state equation is further reduced into

$$\frac{\mathrm{d}\bar{\boldsymbol{\Delta}}(\zeta)}{\mathrm{d}\zeta}=\bar{\boldsymbol{M}}(\zeta)\bar{\boldsymbol{\Delta}}(\zeta)+\bar{\boldsymbol{\Theta}}(\zeta)\boldsymbol{t}_0(\zeta), \tag{9}$$

where $\bar{\boldsymbol{\Delta}}$ is the state vector with pre-incorporated boundary conditions, and the matrices $\bar{\boldsymbol{M}}$ and $\bar{\boldsymbol{\Theta}}$ are obtained by modifying the coefficient matrices in Eq.(7) according to the boundary conditions.

ALM AND SOLUTIONS

Note that Eq.(9) is a differential equation with a variant coefficient matrix, for which a direct solution is rather difficult to achieve. Hence, the ALM (Chen *et al.*, 2003b) is adopted here, in which the plate is divided into p artificial layers, each with a small thickness h_j. Then, each layer is regarded as homogeneous having constant material properties the same as those at the mid-plane of that layer, i.e.,

$$E_j=E(\zeta_{\mathrm{m}}^{(j)}),\ \nu_j=\nu(\zeta_{\mathrm{m}}^{(j)}),\ \alpha_j=\alpha(\zeta_{\mathrm{m}}^{(j)}), \tag{10}$$

where $\zeta_{\mathrm{m}}^{(j)}=(\zeta_{j+1}+\zeta_j)/2$ (j=1, 2, …, p) is the coordinate of the mid-plane of the jth layer. With the above treatment, Eq.(9) is then reduced to one with constant coefficients for the jth layer:

$$\frac{\mathrm{d}\bar{\boldsymbol{\Delta}}^{(j)}(\zeta)}{\mathrm{d}\zeta}=\bar{\boldsymbol{M}}_j\bar{\boldsymbol{\Delta}}^{(j)}(\zeta)+\bar{\boldsymbol{\Theta}}_j\boldsymbol{t}_0(\zeta), \tag{11}$$

for j=1, 2, ⋯, p. The general solution to Eq.(11) is readily sought as

$$\bar{\boldsymbol{\Delta}}^{(j)}(\zeta)=\mathrm{e}^{(\zeta-\zeta_j)\bar{\boldsymbol{M}}_j}\bar{\boldsymbol{\Delta}}^{(j)}(\zeta_j)+\int_{\zeta_j}^{\zeta}\mathrm{e}^{(\zeta-\tau)\bar{\boldsymbol{M}}_j}\bar{\boldsymbol{\Theta}}_j\boldsymbol{t}_0(\zeta)\mathrm{d}\tau, \tag{12}$$

where $\zeta_j\le\zeta\le\zeta_{j+1}$. Since Eq.(12) is valid throughout the kth layer, the transfer relation between the state vectors at the two surfaces of the jth layer is straightforward by setting $\zeta=\zeta_{j+1}$ in Eq.(12). Considering the continuity conditions at the artificial interfaces, the

state vectors at these interfaces can be eliminated based on the transfer matrix method, and hence the global transfer relation between the state vectors on the top (ζ=1) and bottom (ζ=0) surfaces of the plate is obtained as

$$\bar{\boldsymbol{\Delta}}_{\mathrm{t}}^{(p)} = \boldsymbol{T}\bar{\boldsymbol{\Delta}}_{\mathrm{b}}^{(1)} + \boldsymbol{H}, \tag{13}$$

where the subscripts 't' and 'b' indicate the top and bottom surfaces, respectively, and $\boldsymbol{T}$ and $\boldsymbol{H}$ are the global transfer matrix and the thermal load vector, determined by

$$\boldsymbol{T} = \prod_{j=p}^{1} \mathrm{e}^{(\zeta_{j+1}-\zeta_j)\bar{\boldsymbol{M}}_j},$$
$$\boldsymbol{H} = \sum_{j=1}^{p}\left(\prod_{r=p}^{j+1}\mathrm{e}^{(\zeta_{r+1}-\zeta_r)\bar{\boldsymbol{M}}_r}\right)\int_{\zeta_j}^{\zeta_{j+1}}\mathrm{e}^{(\zeta_{j+1}-\tau)\bar{\boldsymbol{M}}_j}\bar{\boldsymbol{\Theta}}_j\boldsymbol{t}_0(\tau)\mathrm{d}\tau. \tag{14}$$

At this stage, if introducing the traction conditions at the two lateral surfaces into Eq.(13), the displacement vectors on the bottom surface can be solved, and hence the state vectors at an arbitrary level ζ are readily derived with repeated use of Eq.(12) together with the continuity conditions.

EFFECTIVE MATERIAL PROPERTIES AND TEMPERATURE FIELD

Functionally graded materials are always manufactured by mixing two different material phases, say metal and ceramic. A good many methods are available to determine effective elastic moduli of such composite materials. Although analytical functions, such as the exponential and power law functions, facilitate obtaining exact solutions for FGMs, they may fail to describe the physical variation of material properties in most FGMs. The rule of mixtures again does not account for the interaction between phases, hence, yielding very approximate values for most of the effective moduli for FGMs. The Mori-Tanaka model (Mori and Tanaka, 1973), developed from the micromechanical level, accounts for the interactions and uses a certain representative volume element to solve the average local stress and strain fields of the constituents of the composite. Here, this model is adopted to determine the effective bulk modulus K_{e} and the effective shear modulus μ_{e} from the following relations:

$$\frac{K_{\mathrm{e}}(z)-K_1}{K_2-K_1} = \frac{V_2(z)}{1+V_1(z)(K_2-K_1)/(K_1+4\mu_1/3)}, \tag{15}$$

$$\frac{\mu_{\mathrm{e}}(z)-\mu_1}{\mu_2-\mu_1} = \frac{V_2(z)}{1+\dfrac{V_1(z)(\mu_2-\mu_1)}{\mu_1+\mu_1(9K_1+8\mu_1)/[6(K_1+2\mu_1)]}}, \tag{16}$$

where K_1, μ_1, and $V_1(z)$ are the bulk modulus, shear modulus and volume fraction of phase 1, respectively, and K_2, μ_2, and $V_2(z)$=1−$V_1(z)$ the corresponding quantities of phase 2. The Young's modulus and Poisson's ratio of the composites are related to the bulk and shear moduli by

$$K = \frac{E}{3(1-2\nu)}, \quad \mu = \frac{E}{2(1+\nu)}. \tag{17}$$

The effective coefficient of linear thermal expansion α_{e} is determined by Rosen and Hashin (1970)'s model as

$$\frac{\alpha_{\mathrm{e}}(z)-\alpha_1}{\alpha_2-\alpha_1} = \frac{1/K_{\mathrm{e}}(z)-1/K_1}{1/K_2-1/K_1}. \tag{18}$$

The effective thermal conductivity k_{e} is determined by Hatta and Taya (1985)'s model as

$$\frac{k_{\mathrm{e}}-k_1}{k_2-k_1} = \frac{V_2(z)}{1+V_1(z)(k_2-k_1)/(3k_1)}. \tag{19}$$

The temperature distribution within the plate is assumed to satisfy the following steady-state thermal conduction without heat supply:

$$k(z)\left(\frac{\partial^2 T}{\partial x^2}+\frac{\partial^2 T}{\partial y^2}\right)+\frac{\mathrm{d}}{\mathrm{d}z}\left[k(z)\frac{\mathrm{d}T}{\mathrm{d}z}\right]=0, \quad q_i = k(z)\frac{\partial T}{\partial x_i}, \tag{20}$$

where $k(z)$ is the thermal conductivity, q_i is the heat flux along the x_i-direction (x_i=x, y, or z). The solution of the temperature field is taken similarly to that for the mechanical and displacement fields in the former formulations and hence the details are omitted here for brevity.

NUMERICAL EXAMPLES

In practical service conditions, FGMs are commonly used in a high-temperature environment with a ceramic top layer as the thermal barrier to a metallic structure. Here, the FGM is assumed to be composed of the two constituent materials, SiC and Al, with the following material properties (Tanaka *et al*., 1993):

$$E_c=427\ \text{GPa},\ \nu_c=0.17,\ \alpha_c=4.3\times10^{-6}\ \text{K}^{-1},$$
$$k_c=65\ \text{W/(m·K)},\ \text{for SiC}, \tag{21a}$$
$$E_m=70\ \text{GPa},\ \nu_m=0.3,\ \alpha_m=23.4\times10^{-6}\ \text{K}^{-1},$$
$$k_m=233\ \text{W/(m·K)},\ \text{for Al}. \tag{21b}$$

In the present analysis, the volume fraction of ceramics is assumed to be given by the following power law function:

$$V_c=V_c^-+(V_c^+-V_c^-)(z/h)^\rho, \tag{22}$$

where V_c^+ and V_c^- are the volume fraction of the ceramic phase on the top and bottom surfaces of the plate, respectively, and ρ is the gradient index indicating the volume fraction profile through the thickness. As proved by Chen *et al.*(2003b) and Lü *et al.*(2006), the ALM will deliver sufficiently accurate results for FGMs with more than twenty artificial layers, due to which forty layers are used in the following calculations.

As illustrating examples, the combination of clamped (C) and simple supports (S) at the edges of $x=0$ and $x=a$ are considered, for which the boundary conditions, in discrete form, are expressed as

$$\text{S: } X_i=V_i=W_i=0, \tag{23a}$$
$$\text{C: } U_i=V_i=W_i=0, \tag{23b}$$

where $i=1$ (for $\xi=0$) or $i=N$ (for $\xi=1$). For all examples, the widely used unequal spaced sampling points proposed by Sherbourne and Pandey (1991) are adopted. The physical quantities involved in the following text are given in the non-dimensional forms as:

$$\overline{T}=\frac{T}{T^+},\ \overline{q}_3=-\frac{q_3h}{k_mT^+},\ \overline{u}=\frac{10l_aU}{\alpha_mT^+},\ \overline{w}=\frac{100l_a^2W}{\alpha_mT^+},$$
$$(\overline{\sigma}_x,\overline{\tau}_{xy})=\frac{10(\sigma_x,\tau_{xy})}{E_m\alpha_mT^+},\ \overline{\tau}_{xz}=\frac{100\tau_{xz}}{E_m\alpha_mT^+l_a},\ \overline{\sigma}_z=\frac{100\sigma_z}{E_m\alpha_mT^+l_a^2}, \tag{24}$$

where the superscript '+' denotes the surface of $z=h$.

Firstly, the thermal deformation of a fully simply supported (SSSS) square plate is considered, which is subjected to a temperature field of $T=T(z)\sin(l_1x)\times\sin(l_2y)$, where $l_1=h/a$, $l_2=h/b$, with the bottom surface held at the reference temperature, i.e., $\hat{T}(0)=0$. Table 1 shows that the temperature, heat flux,

Table 1 Numerical comparisons for temperature, heat flux, displacements, and stresses at specific locations in the SSSS Al/SiC FGM square plate under thermal load (V_c^+=0.5, V_c^-=0, ρ=2, N=9)

Condition		$\overline{T}\left(\frac{a}{2},\frac{a}{2},\frac{h}{2}\right)$	$\overline{q}_3\left(\frac{a}{2},\frac{a}{2},0\right)$	$\overline{u}\left(0,\frac{a}{2},h\right)$	$\overline{w}\left(\frac{a}{2},\frac{a}{2},\frac{h}{2}\right)$	$\overline{w}\left(\frac{a}{2},\frac{a}{2},h\right)$
a=5h	Present	0.3938	0.7316	−1.2106	3.2524	4.414
	Analytical	0.3938	0.7316	−1.2101	3.2497	4.4111
a=10h	Present	0.4240	0.8075	−1.2129	3.3337	3.6362
	Analytical	0.4240	0.8075	−1.2124	3.3312	3.6337
a=40h	Present	0.4343	0.8335	−1.2136	3.3591	3.3783
	Analytical	0.4343	0.8335	−1.2131	3.3567	3.3758
Condition		$\overline{\sigma}_x\left(\frac{a}{2},\frac{a}{2},h\right)$	$\overline{\tau}_{xy}(0,0,h)$	$\overline{\tau}_{xz}\left(0,\frac{a}{2},\frac{3h}{4}\right)$	$\overline{\sigma}_z\left(\frac{a}{2},\frac{a}{2},\frac{h}{2}\right)$	
a=5h	Present	−4.1715	−6.4833	4.2383	−8.6577	
	Analytical	−4.1764	−6.4804	4.2264	−8.6829	
a=10h	Present	−4.1509	−6.4955	4.4825	−9.1362	
	Analytical	−4.1555	−6.4928	4.4703	−9.1622	
a=40h	Present	−4.1447	−6.4992	4.5624	−9.2928	
	Analytical	−4.1492	−6.4966	4.5501	−9.3191	

displacements, and stresses at specific locations obtained by the present semi-analytical method are in excellent agreement with the analytical solutions by Vel and Batra (2002) using the power series expansion.

Secondly, the convergence properties of the present method for non-fully simply supported plates are to be clarified. Table 2 presents the numerical results of temperature, heat flux, displacements, and stresses at specific locations in SCSC and SCSS square plates with various discrete point numbers. Obviously the present method, irrespective of the change in boundary conditions, converges rapidly with the increasing sampling point number in the DQ procedure.

Thirdly, the effects of gradient index ρ on the thermo-mechanical behavior of FGM square plates are investigated. Fig.1 gives the through-thickness distributions of displacements and in-plane stresses for SCSC (lines with circles) and SSSS (lines without circles) plates with $V_c^+=1$, $V_c^-=0$, and a/h=5 for various gradient index ρ. Note that the case of ρ=0 corresponds exactly to the homogeneous SiC plate as indicated in Eq.(21) for the present values of V_c^+ and V_c^-. Fig.1 shows that SCSC and SSSS plates behave similarly with different quantity amplitudes for the same value of ρ. In general, the displacements and the in-plane shear stresses for SSSS plates are larger than those of SCSC plates, while it is the contrary for the in-plane normal stresses. The in-plane displacement $\bar{u}$ for the SSSS plate increases monotonically as ρ increases. By contrast for $\bar{u}$ of the SCSC plate, only that within $0.25<\zeta<1$ exhibits the same phenomenon, and that within $0<\zeta<0.25$ decreases when ρ increases from 0 to 0.5, and then increases with a negative sign as ρ increases from 2 to 4. In comparison, the deflection does not vary following a uniform rule. As for the stresses, the nonlinearity becomes increasingly obvious when ρ increases. A special phenomenon is observed for the in-plane normal stresses (Fig.1c), namely that the curves experience a drastic bend within $0.8\leq\zeta\leq1$ when ρ=2 and ρ=4. Moreover, the larger the value of ρ, the more drastic the variation the stress undergoes, with the SSSS plate bearing tensile stress in the vicinity of the top surface when ρ=4.

Finally, the effects of variations of the volume fraction of SiC on the thermomechanical behavior of FGM square plates (a/h=5) are discussed. Fig.2 plotted the variations of displacement $w(0.5a, 0.5a, h)$ and stress $\sigma_x(0.5a, 0.5a, h)$ of SSSS (lines without circles) and SCSC (lines with circles) plates vs the volume fraction V_c^+ of SiC (V_c^-=0) on the top surface for different gradient indices ρ. In the plot, the ordinate represents the relative increment of the quantities of FGM plates against those (w_0 or σ_{x_0}) of the homogeneous Al plates (V_c^+=0). It is observed from Fig.2a that the displacements decrease almost linearly as V_c^+ increases for all considered gradient indices, with a maximal decrement of more than 80% when V_c^+=1. Comparatively, the variation of normal stress σ_x against V_c^+ exhibits an obvious non-linear behavior. Except in the case of ρ=2 for SSSS plate, for which the normal stress decrease monotonically as V_c^+ increases, all other stresses increase first and then decrease at

Table 2 Convergence of the present method for displacements and stresses at specific locations in the Al/SiC FGM square plate under thermal load (V_c^+=1, V_c^-=0, ρ=0.5, a/h=5)

B.C.	N	$\bar{T}\left(\frac{a}{2},\frac{a}{2},\frac{h}{2}\right)$	$\bar{q}_3\left(\frac{a}{2},\frac{a}{2},0\right)$	$\bar{u}\left(\frac{a}{4},\frac{a}{2},h\right)$	$\bar{w}\left(\frac{a}{2},\frac{a}{2},\frac{h}{2}\right)$	$\bar{\sigma}_x\left(\frac{a}{2},\frac{a}{2},h\right)$	$\bar{\tau}_{xy}\left(\frac{a}{4},\frac{a}{4},h\right)$
SCSC	5	0.3395	0.3905	−0.1208	0.4704	−8.0191	−2.4104
	7	0.3394	0.3903	−0.1242	0.4750	−8.0214	−2.3704
	9	0.3394	0.3903	−0.1232	0.4771	−7.8268	−2.3688
	11	0.3394	0.3903	−0.1241	0.4767	−7.9593	−2.3785
	13	0.3394	0.3903	−0.1241	0.4771	−7.8694	−2.3765
SCSS	5	0.3395	0.3905	−0.1007	0.6698	−5.8576	−2.1917
	7	0.3394	0.3903	−0.1002	0.6625	−6.0330	−2.1410
	9	0.3394	0.3903	−0.0986	0.6645	−5.9085	−2.1421
	11	0.3394	0.3903	−0.0995	0.6639	−5.9911	−2.1522
	13	0.3394	0.3903	−0.0997	0.6642	−5.9347	−2.1503

an ascending speed. The curves in Fig.2 also indicate that, for a given gradient index ρ, as the volume fraction of SiC on the top surface changes, the variations of the transverse displacement are almost the same for SSSS and SCSC plates (Fig.2a), but those of the in-plane normal stress are much different (Fig.2b).

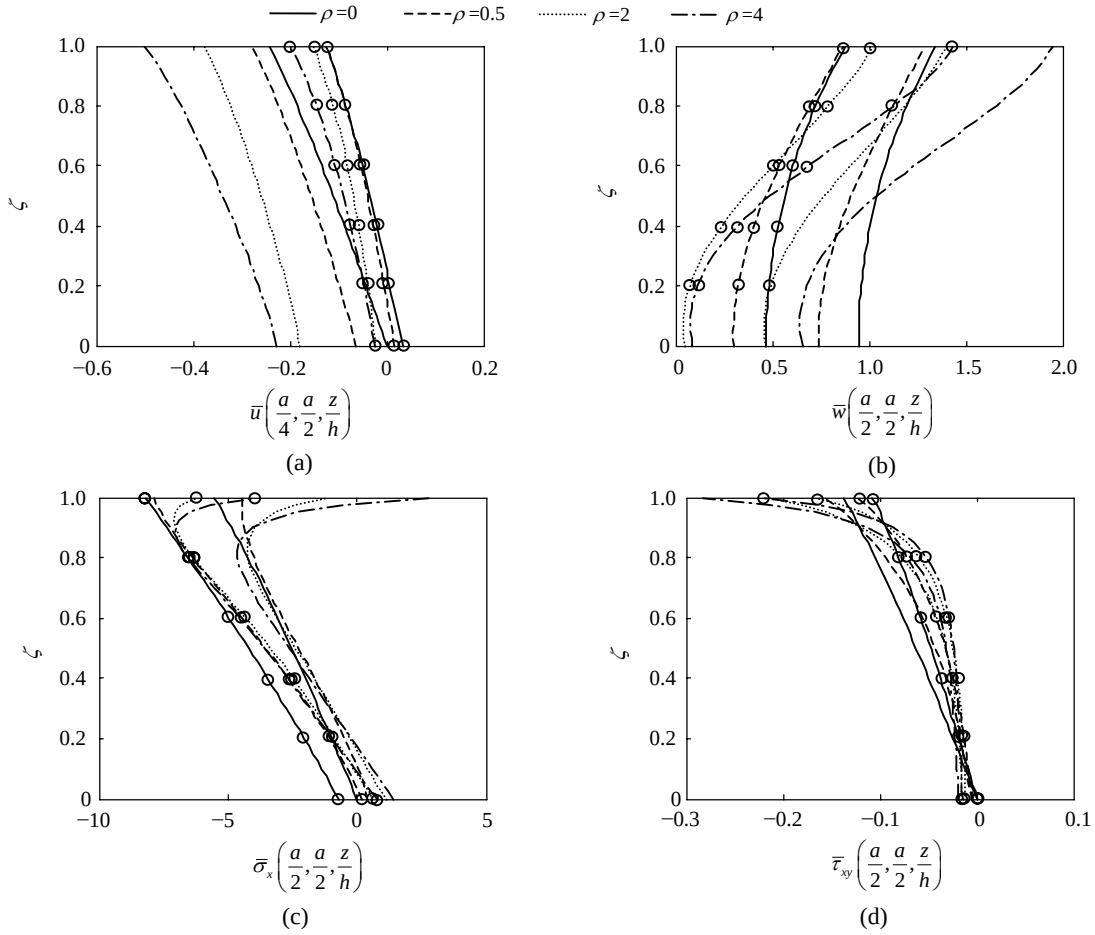

Fig.1 Effects of gradient index ρ on through-thickness distributions of displacement and stresses of SSSS (lines without circles) and SCSC (lines with circles) Al/SiC FGM plates (V_c^+=1, V_c^-=0, a/h=5, N=9). (a) In-plane displacement; (b) Deflection; (c) In-plane normal stress; (d) In-plane shear stress

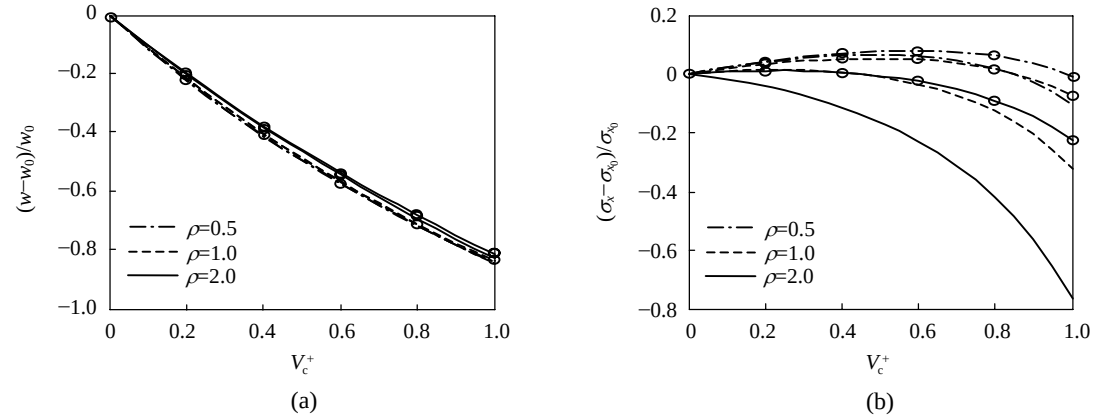

Fig.2 Variations of displacement w(0.5a, 0.5a, h) and stress σ_x(0.5a, 0.5a, h) vs volume fraction of SiC for SSSS (lines without circles) and SCSC (lines with circles) Al/SiC FGM square plates (V_c^-=0, a/h=5, N=9). (a) Deflection; (b) In-plane normal stress

CONCLUSION

Thermal deformations of FGM thick plates are investigated using a semi-analytical method. The analysis is directly based on the 3D theory of elasticity; hence no assumptions about the distributions of displacement and stress are introduced, enabling the current method to be suitable for laminates with arbitrary thickness. The employment of the differential quadrature technique makes it feasible to treat non-simply supported edges, thus expanding the application of the traditional state space method for FGM plates. Although the Mori-Tanaka method is applied to predict the effective moduli of the plate, the ALM in the present work is applicable to arbitrary variations of material properties through the plate thickness. Numerical comparisons solidly validated the present semi-analytical methods, which can therefore serve as an alternative for further analysis of FGM thick plates.

Since FGMs are omnipresent in an extremely high temperature environment, the material properties are always temperature dependent. In such cases, material properties will differ at any arbitrary point with different temperature magnitudes; that is, the plate will be functionally graded not only through the thickness direction but also in the in-plane directions.

Hence, more general decomposition techniques are necessary to achieve the global analysis of the thermomechanical behavior of FGMs. This issue will fall into the scope of the authors' subsequent work.

References

Bellman, R.E., Casti, J., 1971. Differential quadrature and long-term integration. *Journal of Mathematical Analysis and Applications*, **34**(2):235-238. [doi:10.1016/0022-247X(71)90110-7]

Bian, Z.G., Chen, W.Q., Lim, C.W., Zhang, N., 2005. Analytical solutions for single- and multi-span functionally graded plates in cylindrical bending. *International Journal of Solids and Structures*, **42**(24-25):6433-6456. [doi:10.1016/j.ijsolstr.2005.04.032]

Chen, W.Q., Lüe, C.F., 2005. 3D free vibration analysis of cross-ply laminated plates with one pair of opposite edges simply supported. *Composite Structures*, **69**(1):77-87. [doi:10.1016/j.compstruct.2004.05.015]

Chen, W.Q., Lv, C.F., Bian, Z.G., 2003a. Elasticity solution for free vibration of laminated beams. *Composite Structures*, **62**(1):75-82. [doi:10.1016/S0263-8223(03)00086-2]

Chen, W.Q., Bian, Z.G., Ding, H.J., 2003b. Three-dimensional analysis of a thick FGM rectangular plate in thermal environment. *Journal of Zhejiang University SCIENCE*, **4**(1):1-7.

Chen, W.Q., Lv, C.F., Bian, Z.G., 2004. Free vibration analysis of generally laminated beams via state-space-based differential quadrature. *Composite Structures*, **63**(3-4):417-425. [doi:10.1016/S0263-8223(03)00190-9]

Cheng, Z.Q., Batra, R.C., 2000. Three-dimensional thermoelastic deformations of a functionally graded elliptic plate. *Composites Part B: Engineering*, **31**(2):97-106. [doi:10.1016/S1359-8368(99)00069-4]

Ding, H.J., Chen, W.Q., Zhang, L.C., 2006. Elasticity of Transversely Isotropic Materials. Springer, Dordrecht.

Hatta, H., Taya, M., 1985. Effective thermal conductivity of a Misoriented short fiber composite. *Journal of Applied Physics*, **58**(7):2478-2486. [doi:10.1063/1.335924]

Kashtalyan, M., 2004. Three-dimensional elasticity solution for bending of functionally graded rectangular plates. *European Journal of Mechanics-A/Solids*, **23**(5): 853-864. [doi:10.1016/j.euromechsol.2004.04.002]

Koizumi, M., 1997. FGM activities in Japan. *Composites Part B: Engineering*, **28**(1-2):1-4. [doi:10.1016/S1359-8368(96)00016-9]

Lü, C.F., Chen, W.Q., 2005. Free vibration of orthotropic functionally graded beams with various end conditions. *Structural Engineering and Mechanics*, **20**(4):465-476.

Lü, C.F., Chen, W.Q., Zhong, Z., 2006. Two-dimensional thermoelasticity solution for functionally graded thick beams. *Science in China Series G: Physics, Mechanics and Astronomy*, **49**(4):451-460. [doi:10.1007/s11433-006-0451-2]

Lü, C.F., Lim, C.W., Xu, F., 2007. Stress analysis of anisotropic thick laminates in cylindrical bending using a semi-analytical approach. *Journal of Zhejiang University SCIENGE A*, **8**(11):1740-1745. [doi:10.1631/jzus.2007.A1740]

Lü, C.F., Chen, W.Q., Xu, R.Q., Lim, C.W., 2008. Semi-analytical elasticity solutions for bi-directional functionally graded beams. *International Journal of Solids and Structures*, **45**(1):258-275. [doi:10.1016/j.ijsolstr.2007.07.018]

Matsunaga, H., 2008. Free vibration and stability of functionally graded plates according to a 2-D higher-order deformation theory. *Composite Structures*, **82**(4):499-512. [doi:10.1016/j.compstruct.2007.01.030]

Mian, A.M., Spencer, A.J.M., 1998. Exact solutions for functionally graded and laminated elastic materials. *Journal of the Mechanics and Physics of Solids*, **46**(12):2283-2295. [doi:10.1016/S0022-5096(98)00048-9]

Mori, T., Tanaka, K., 1973. Average stress in matrix and average elastic energy of materials with misfitting inclusions. *Acta Metallurgica*, **21**(5):571-574. [doi:10.1016/0001-6160(73)90064-3]

Reddy, J.N., 2000. Analysis of functionally graded plates. *International Journal for Numerical Methods in Engineering*, **47**(1-3):663-684. [doi:10.1002/(SICI)1097-0207(20000110/30)47:1/3<663::AID-NME787>3.0.CO;2-8]

Reddy, J.N., Cheng, Z.Q., 2001. Three-dimensional thermomechanical deformations of functionally graded

rectangular plates. *European Journal of Mechanics-A/Solids*, **20**(5):841-855. [doi:10.1016/S0997-7538(01)01174-3]

Rosen, B.W., Hashin, Z., 1970. Effective thermal expansion coefficients and specific heats of composite materials. *International Journal of Engineering Science*, **8**(2):157-173. [doi:10.1016/0020-7225(70)90066-2]

Sherbourne, A.N., Pandey, M.D., 1991. Differential quadrature method in the buckling analysis of beams and composite plates. *Computers and Structures*, **40**(4):903-913. [doi:10.1016/0045-7949(91)90320-L]

Shu, C., 2000. Differential Quadrature and Its Application in Engineering. Springer-Verlag, London.

Tanaka, K., Tanaka, Y., Enomoto, K., Poterasu, V.F., Sugano, Y., 1993. Design of thermoelastic materials using direct sensitivity and optimization methods. Reduction of thermal stresses in functionally gradient materials. *Computer Methods in Applied Mechanics and Engineering*, **106**(1-2):271-284. [doi:10.1016/0045-7825(93)90193-2]

Tarn, J.Q., Wang, Y.M., 1995. Asymptotic thermoelastic analysis of anisotropic inhomogeneous and laminated plates. *Journal of Thermal Stresses*, **18**(1):35-58. [doi:10.1080/01495739508946289]

Vel, S.S., Batra, R.C., 2002. Exact solution for thermoelastic deformations of functionally graded thick rectangular plates. *AIAA Journal*, **40**(7):1421-1433. [doi:10.2514/2.1805]

Vel, S.S., Batra, R.C., 2003. Three-dimensional thermoelastic analysis of transient thermal stresses in functionally graded plates. *International Journal of Solids and Structures*, **40**(25):7181-7196. [doi:10.1016/S0020-7683(03)00361-5]

Zhong, Z., Shang, E.T., 2003. Three-dimensional exact analysis of a simply supported functionally gradient piezoelectric plate. *International Journal of Solids and Structures*, **40**(20):5335-5352. [doi:10.1016/S0020-7683(03)00288-9]

Zhong, Z., Shang, E.T., 2005. Exact analysis of simply supported functionally graded piezothermoelectric plates. *Journal of Intelligent Material Systems and Structures*, **16**(7-8):643-651. [doi:10.1177/1045389X05050530]